Geotechnical Predictions of the Excavation Disturbed Zone at Stripa

N. Barton
A. Makurat
K. Monsen
G. Vik
L. Tunbridge
Norwegian Geotechnical Institute
(Oslo, Norway)

Abstract

The 3m wide by 2m high by 50m long validation drift at Stripa surprised the site characterisation and validation project investigators, by the limited amount of water inflow compared to borehole measurements and predictions. Rock mechanics characterisation and laboratory and field tests performed by NGI are reviewed in an attempt to explain the reduced inflows. Discrete element UDEC-BB modelling was used to predict the effects of excavation induced disturbance in two-dimensional models. Full coupling of hydro-mechanical effects was incorporated in some models and shown to be important compared to mechanical modelling.

Prédictions géotechniques de la zone perturbée autour d'une excavation à Stripa

Résumé

La galerie d'accés, de trois mètres de large, deux mètres de haut et cinquante mètres de long, à Stripa, utilisée pour les validations, a surpris les enquêteurs chargés de la charactérisation du site et du projet de validation, par le faible débit d'eau comparé aux prédictions et mesures de sondage. La charactérisation de mécanique des roches et les tests in situ et au laboratoire effectués par NGI sont repassés en revue afin d'expliquer les débits réduits. Une modélisation par la méthode des éléments discrets UDEC-BB a été effectuée pour prédire les effets de perturbation induite par l'excavation dans des modèles à deux dimensions. Le couplage des effets hydro-mécaniques a été incorporé dans certains modèles et se révèle important comparé aux cas où la modélisation est purement mécanique.

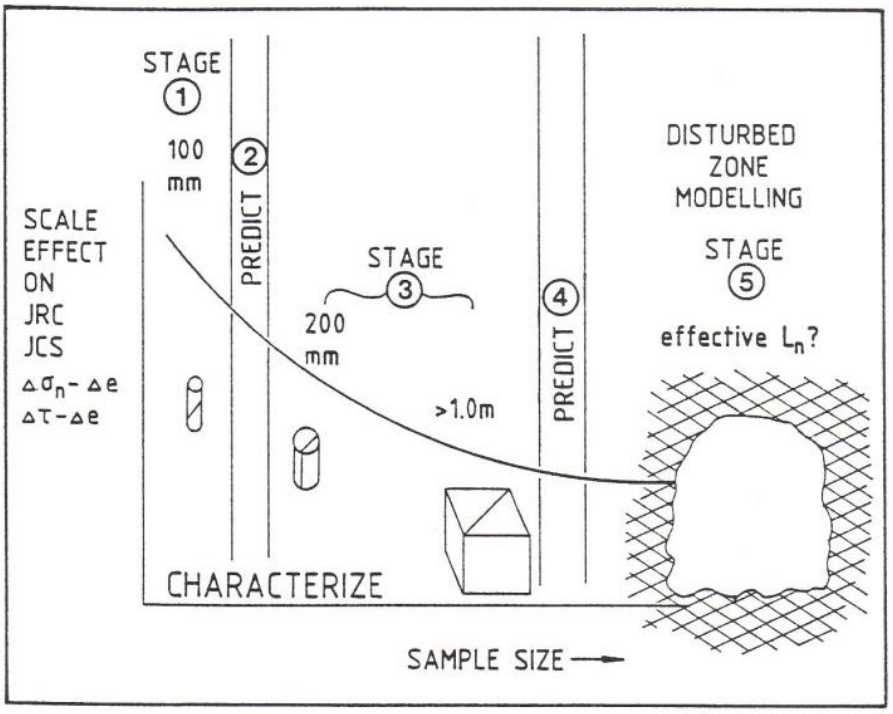

Fig. 1. Five stages of joint characterisation and prediction.

INTRODUCTION

The relatively small 3m wide by 2m high validation drift at Stripa has surprised modellers by the limited water inflow recorded. Suggested reasons for the reduced inflow compared to that recorded in peripheral boreholes have included blast vibration and blast gas effects, stress redistribution causing reduced radial permeability, shear displacements on joints, and two phase flow conditions due to degassing of the groundwater.

Rock mechanics tests and numerical modelling were included in the Site Characterisation and Validation project, in the hope of gaining some insight into the mechanical processes caused by tunnel excavation. However, the rock mechanics modelling was not incorporated in the Fracture Flow Task Force modelling nor in the planning of the validation drift inflow experiment.

STAGE BY STAGE CHARACTERISATION

A schematic presentation of the various stages of the rock mechanics test programme is given in Fig. 1. Joints were characterised at successively larger scales and in smaller numbers, as Stage 1 passed into Stage 3.

- Stage 1 201 joints 100mm diameter core (NGI)
- Stage 3 5 joints 200mm core (NGI, MUN, LULEÅ)
- Stage 3 1 joint 1000 × 1000mm block test (NGI)

Coupled stress-flow tests were performed at 200mm scale in NGI (Makurat et al., 1990a) and in the Memorial University of Newfoundland by Gale et al.,

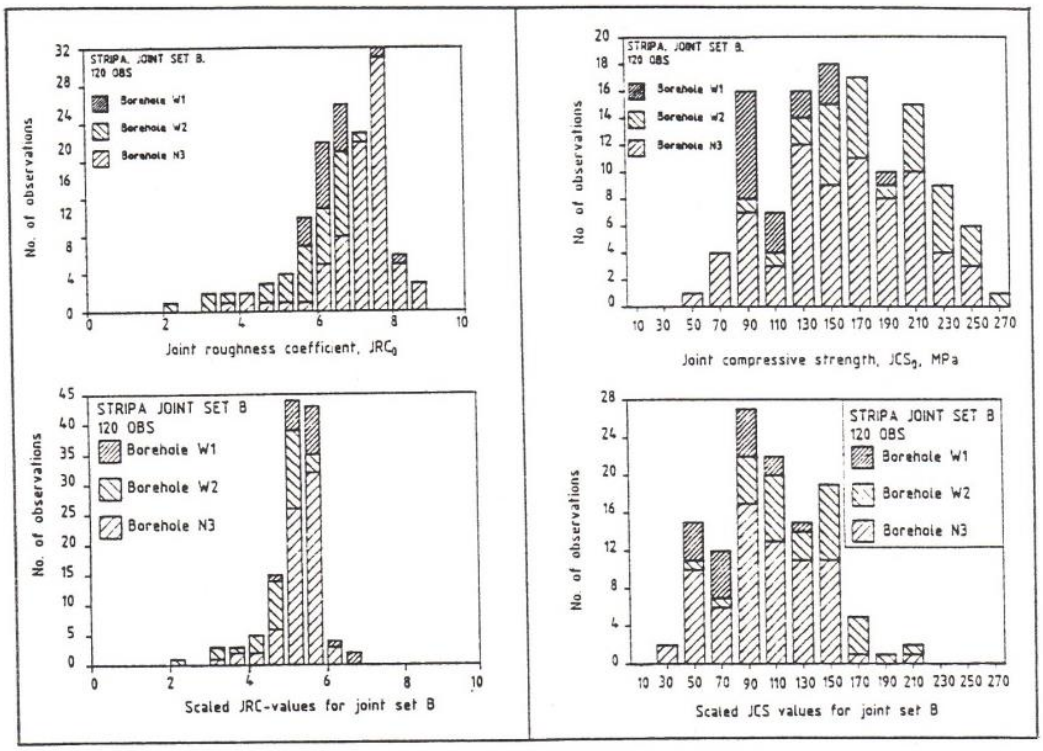

Fig. 2. Examples of JRC and JCS statistics for Stripa SCV joint set B, showing block size scaling from 100mm core to assumed 0.5m block in situ. (Vik and Johansen, 1990)

1990a (TR 90-11), and at the Technical University of Luleå by Hakami, 1989 (TR 89-08).

Stage 1: Characterisation

Joints recovered in drill core from some of the first exploratory holes W1, W2 and B3 were selected for characterisation. One hundred and twenty-two joints represented the N-S trending Set A, while fifty-two joints represented the NW-SE trending Set B. A further twenty-seven joints were tested that were not matched with one of the sets identified by Gale and Stråhle, 1988 (TR 88-10).

The Stage 1 tests were purely mechanical; utilising tilt (very low gravity-induced shear and normal stress) index tests to characterise joint roughness (JRC), and Schmidt hammer rebound testing to characterise joint wall strength (JCS). As indicated in Fig. 1, these parameters are sample size dependent, declining in value as block size or joint length is increased. The peak friction angle (ϕ) can be predicted as follows (Barton and Choubey, 1977):

$$\phi = JRC \log\left(\frac{JCS}{\sigma_n}\right) + \phi_r$$

where JRC = joint roughness coefficient, JCS = joint wall compression strength, and ϕ_r = residual friction angle. Stress-closure behaviour is also strongly governed by JRC and JCS values (Bandis et al., 1983).

Fig. 2 shows histograms of the measured data for joint roughness (JRC) and wall strength (JCS), and conversion to values appropriate to *in situ* block sizes (Barton and Bandis, 1982). Table 1 gives median values of the key joint strength parameters with example values of predicted peak friction angles for assumed normal stress levels of 5 and 25 MPa ($\phi_5{}^\circ$ and $\phi_{25}{}^\circ$).

Table 1. **Predicted median values of joint strength parameters for stripa joints (approximately 100mm scale). JCS in units of MPa.**

Joint Set	JRC	JCS	$\phi_r{}^\circ$	$\phi_5{}^\circ$	$\phi_{25}{}^\circ$
B (N-S strike)	6.4	140	25.5°	35.5°	30.7°
A (NW-SE strike)	7.1	120	24.3°	34.1°	29.1°

The values of JCS ranged from 60 to 220 MPa, and ϕ_r ranged from 20° to 30°, reflecting the effect of several mineral fillings and coatings in the various sets. In general, joint roughness showed more uniformity.

Stage 2: Prediction

With the assumed *in situ* block size of 0.5m, corrected "full-scale" values for JRC_n were 5.3 and 5.4, while "full-scale" values of JCS_n were 95 and 80 MPa for sets B and A respectively (Fig. 2 shows examples).

The above input data was used in the Barton-Bandis joint sub-routine (which is part of the discrete element model UDEC-BB) to generate sets of joint behaviour curves for the following variables:

A) shear strength - displacement B) dilation - displacement
C) conductivity - displacement D) normal stress - closure
E) normal stress - conductivity.

The predicted behaviour for joints with the median strength parameters given in Table 1 is reported in Vik and Barton, 1988 (TR 88-08). Sketches of the general form of these five sets of behaviour curves are given in Fig. 3 (A to E).

Stage 3a: CSFT Coupled Stress-Flow Testing of 200mm Cores

Coupled stress-flow testing was performed in NGI's biaxial CSFT apparatus, on two joints recovered from 200mm drillcore. Test I was performed on a planar, mineralized joint representing Set B (N-S strike) from the 2D drift. Test II was performed on a nearly planar, mineralized joint representing Set A (NW-SE strike) from the 3D drift. This core was taken from the same joint that formed the diagonal to the 1m × 1m × 2m *in situ* block test. Table 2 gives the mean values obtained from tilt and Schmidt

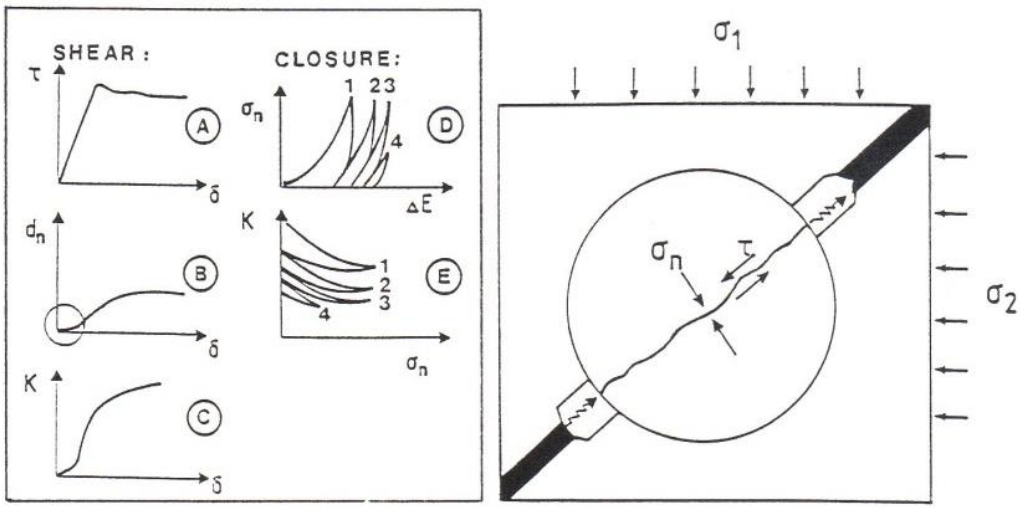

Fig. 3. Shear-dilation-permeability and stress-closure-permeability coupling and their measurement in CSFT tests.

hammer tests on these larger 200mm joint samples (from parts of the same joint, immediately adjacent to the CSFT sample).

Table 2. **Approximate values of joint strength parameters for the 200mm CSFT test (JCS_n in units of MPa).**

Joint Set	Sample	JRC_n	JCS_n	ϕ_r
B (N-S strike)	No. 1	1.9	150	26.5°
A (NW-SE strike)	No. 2	3.8	125	25.1°

Table 2 indicates that the two large core samples had fairly typical JCS and ϕ_r values, representative of the mineralized nature of many of the joints at Stripa. However, the planarity (and probably the persistence) were approaching extreme values.

i) Stress - Closure - Flow testing

The effect of the three normal stress cycles to 25 MPa on conducting apertures is illustrated in Fig. 4. Initial (unloaded) apertures reduced from 175μ to below 15μm for sample No. 1 ($JRC_n \approx 1.9$) and from 285μm to about 30μm for sample No. 2 ($JRC_n \approx 3.8$). The measurement of smaller initial and final apertures for smoother joints was consistent with previous experience and with predictions (Barton et al., 1985).

ii) Shear - Dilation - Flow testing

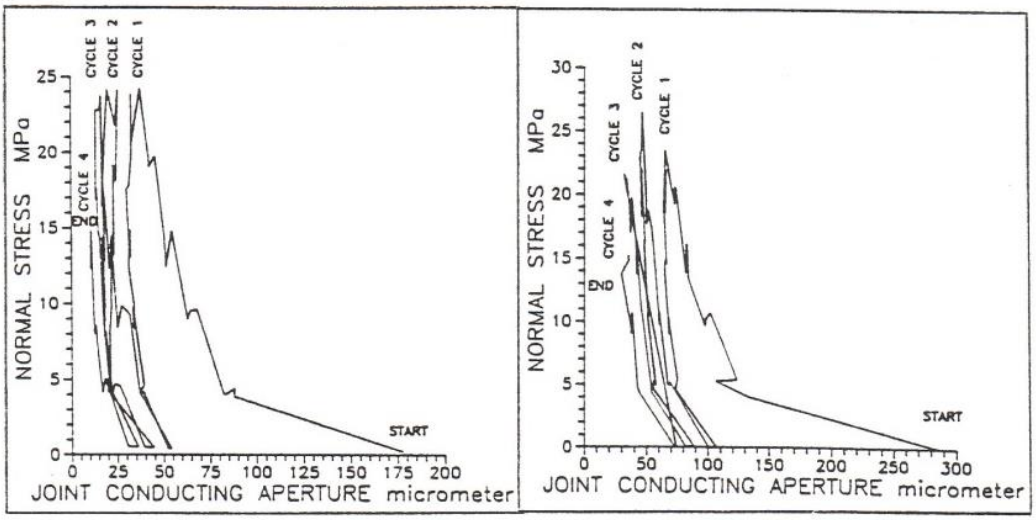

Fig. 4. Normal loading effect on conducting apertures measured in joint samples 1 and 2; 200mm cores. (Left: Set B, N-S, JRC_n = 1.9, and Right: Set A, NW-SE, JRC_n = 3.8.)

Three shearing increments were subsequently applied to give shear displacements of approximately 0.3mm, 1.0 - 1.2mm and 2.0 - 2.3mm. The first shear increments appeared to cause no increase in conducting aperture, and may, as in the case of joint No. 2, cause a reduction if the normal stress increases during the shearing event. In the next shear increment from approximately 0.3mm to 1.0 or 1.2mm, a consistent increase in conducting aperture was measured in both tests. This increment caused conducting apertures to increase from approximately 8 to 16μm in joint No. 1, and from approximately 15 to 30μm in joint No. 2. Normal stress was held at a high level (23 to 28 MPa) throughout this increment.

Conductivity reduced in the static period following several of the shearing increments under high normal stress, possibly due to the action of creep in the chlorite coatings. *This type of behaviour is also likely to have occurred in the validation drift.*

Stage 3b: CSFT Coupled Stress Flow Testing of 2m^3 Block

The final step in the rock mechanics test programme was the performance of an *in situ* block test. The persistent, chlorite-coated joint that was sampled in test No. 2 at 200mm scale, was selected as a diagonal in the 1m × 1m × 2m block test. It was therefore sampled at 1400mm scale. The test was performed in the 3D drift, north of the cross and close to the west wall of the drift. The block was loaded with pairs of 1m^2 flatjacks placed within steel boxes that were cemented into core-drilled slots on the four sub-vertical sides of the block. Fig. 5 shows the test set-up.

The undisturbed joint (prior to flatjack slot drilling) was permeability tested

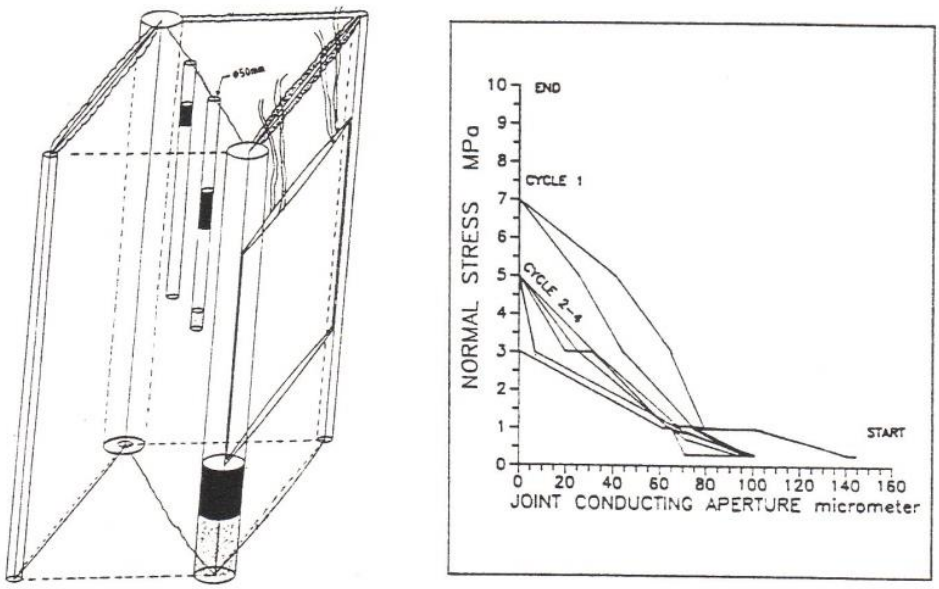

Fig. 5. In situ block test for coupled stress, shear, flow testing of joint Set A (as CSFT No. 2). NGI performed this 1 × 1 × 2 × m test in the N end of the 3D Migration drift.

by a small scale crosshole procedure, and indicated conducting apertures (e) in the range of 5 to 7μm. Following the unloading caused by the drilling of the flatjack slots (2m in depth), the conducting aperture increased to 145μm.

During four load cycles to 10 MPa normal stress (Fig. 5), the conducting aperture reduced to zero (non-measurable) on each cycle. On Cycles 1 and 2, normal stresses of 5 to 7 MPa were sufficient; on Cycles 3 and 4, normal stresses of 3 to 5 MPa were sufficient.

The measured physical closures (ΔE) on each cycle were 98μm, 43μm and 8μm, respectively. Just prior to commencement of shearing on the fourth cycle, the joint had physically closed a total of 95μm (= ΔE). However, the original (unloaded) conducting aperture of 145μm had reduced to zero (unmeasurable flow) (= Δe). This suggests some physical changes in the flow path, perhaps caused by the deformable chlorite fill. *Such behaviour is likely to have occurred in the validation drift, with its numerous mineralized joints.*

Shearing of up to 1.8mm was achieved under a normal stress of 10 to 11 MPa. No flow was registered during any of the shearing events. A measured joint dilation of only 8μm occurred during the first 360μm of shear. Thereafter, a continuous reduction of physical aperture was measured during shear, amounting to some 10μm. The joint, as measured at this 1400mm scale, was clearly too planar to dilate significantly, and was effectively sealed to water flow at a moderate normal stress level, perhaps due to "damage" to pre-existing flow channels in the chlorite infill.

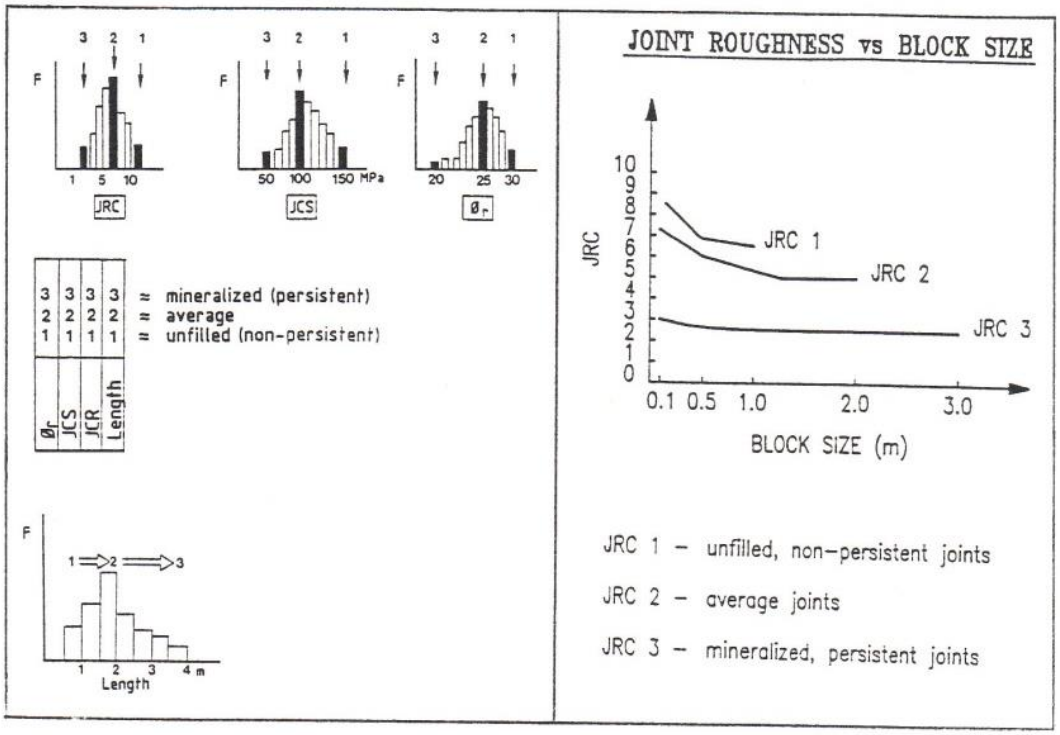

Fig. 6. The relevant values of JRC, JCS and ϕ_r were chosen with respect to joint length, with lower values for the persistent mineralized joints.

Stage 4: Predicting Input Data for Numerical Modelling

As shown in Fig. 2, the characterisation data for the joints was organised in the form of histograms, so that the variability of the parameters JRC (Joint Roughness Coefficient), JCS, (Joint Wall Compressive Strength) and ϕ_r (Residual Friction Angle) was accounted for. The first four UDEC-BB models utilised mean values of these input parameters (material model 2 "average") in the histograms sketched in Fig. 6, while models 5, 6, 7 and 8 (with unchanged joint structures) utilised three sets of length-dependent values of the joint strength parameters.

The shortest joints were therefore given high values to represent rough, interlocked, higher stiffness behaviour. Joints of intermediate length were given intermediate properties. The more persistent mineralized joints were given the lowest values of JRC, JCS and ϕ_r.

Table 3 gives the final form of the input data for the joints as required for the Stage 5 UDEC-BB studies. Definition of terms are given on the right-hand side of the table.

The one-dimensional joint behaviour was calculated by use of a Lotus spreadsheet version of the Barton-Bandis joint model (see Makurat et al., 1990b). The joint conductivity vs shear displacement behaviour predicted for the three joint models is shown in Fig. 7. Note that the physical aperture (E)

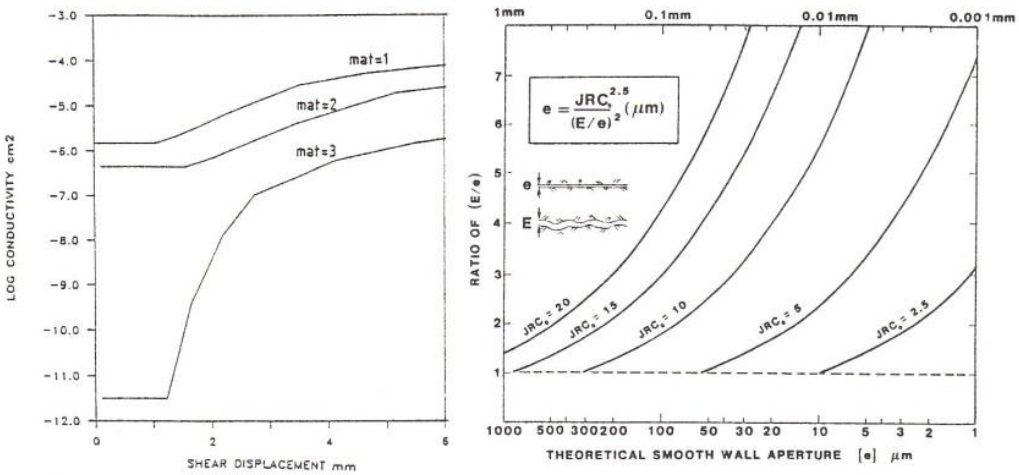

Fig. 7. (Left) Prediction of shear-dilation-conductivity coupling for the three joint material models. (Right) Method of converting physical joint apertures (E) to conducting apertures (e).

is converted to the conducting aperture (e) by the empirical model shown in Fig. 7 (Barton, 1982). The intact rock was modelled as an elastic isotropic medium acting under plane strain conditions, with elastic properties as listed in Table 4.

Table 3. **Joint material input parameters.**

parameter	unit	mat = 3	mat = 2	mat = 1	explanation
L	m	L > 2	1 < L < 2	L < 1	joint length
JRC_0		3.0	7.25	8.5	joint roughness coefficient, lab. scale
JCS_0	MPa	70	140	200	joint wall compressive strength, lab. scale
L_0	m	0.1	0.1	0.1	block size, lab. scale
L_n	m	1.0	1.0	0.5	block size, *in situ*
ϕ_r	°	21	25	29	residual angle of friction
σ_c	MPa	240	240	240	uniaxial compressive strength
JKN	$\frac{GPa}{mm}$	1.3e7	7.2e7	7.1e10	joint normal stiffness limit
JKS	$\frac{GPa}{mm}$	8.4e3	8.2e3	14.3e3	joint shear stiffness limit
E_0	mm	0.100	0.100	0.100	zero stress aperture

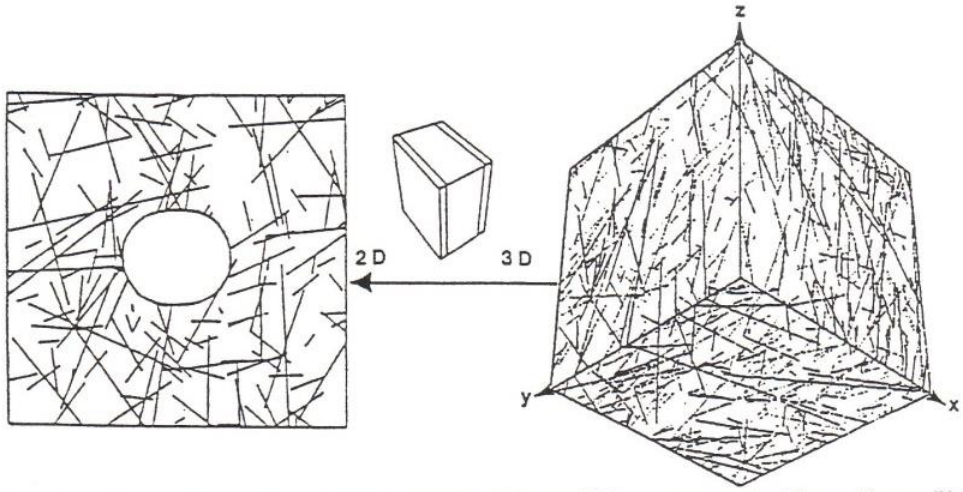

Fig. 8. Two-dimensional jointed (UDEC-BB) models were created from Harwell's 8m × 8m × 8m stochastically generated cubes. (Herbert, 1989)

Table 4. **Intact rock material input parameters.**

parameter	parameter	No.	units
density of rock	γ	2600	kg/m^3
bulk modulus	K	38.0	GPa
shear modulus	G	22.8	GPa

Bulk and shear moduli of the intact rock have been calculated based on classical theory of elasticity. Young's modulus E = 57 GPa and Poisson's ratio v = 0.25 gives:

$$Bulk\ modulus : K = \frac{E}{3(1-2\nu)} = 38.0\ GPa$$

$$Shear\ modulus : G = \frac{E}{2(1+2\nu)} = 22.8\ GPa$$

Stage 5: Discrete Element (UDEC-BB) Modelling

UDEC-BB is a two-dimensional version of the distinct element method which is specifically designed to simulate the predominant features of naturally jointed or of fractured rock masses, including:

- variable rock deformability
- complex joint structures
- non-linear, inelastic joint behaviour
- fluid flow in joints
- far-field static or dynamic boundary conditions
- transient heat flow and thermally-induced stresses

The BB subroutine simulating the behaviour of joints has the following major features:

1) hyperbolic normal closure function (joint stiffness increases with closure) (Bandis et al., 1983);
2) closure limit (joints cannot continue to close at very high normal stress);
3) normal reversal logic (an unloaded joint will experience hysteresis, and will stiffen each time it is reloaded);
4) joint opening (if the joint is pulled apart, stiffness is reduced to that of disturbed joint conditions upon reloading);
5) shear reversal and damage (shear stiffness of joint depends on number of reversals and extent of shear displacement) (Barton et al., 1985);
6) dilation with shear; joint dilation is a function of shear displacement and normal stress, joint normal stiffness decreases with shear and dilation.
7) The calculated physical joint apertures (E) resulting from joint closure, opening, shear and dilation are converted to conducting apertures (e) for flow calculations as shown in Fig. 7.

The UDEC code was developed by Cundall (1980), and its application as UDEC-BB with the Barton-Bandis joint logic is described by Makurat et al. (1990b). The BB joint logic is described by Barton et al. (1985), and Bandis et al. (1981; 1983).

Modelled joint geometries

Systematic joint mapping performed by Gale et al., 1990b (IR 90-02) provided the statistical data for Harwell's initial 8m × 8m × 8m stochastically generated jointed cubes (Herbert, 1989). The four appropriate end faces of these two cubes were used by NGI to define possible discrete two-dimensional joint geometries for rock mechanics modelling. One of the stochastic models and an end face are illustrated in Figure 8 (Herbert, 1989).

The modelling, all of which was predictive in nature, was divided into four stages:

I Modelling with average joint material parameters, Models 1, 2, 3 and 4
II Modelling with length-dependent joint material parameters, Models 5, 6, 7 and 8 (see Fig. 9)
III Comparison with continuum analyses
IV Hydromechanical (coupled) D-hole and validation drift inflow modelling using Models 5 and 8.

For the most part, only two joint sets (A and C) were represented in the eight UDEC-BB models. Set B crossing the future drift direction nearly at right angles could not be modelled by UDEC, but was represented in Itasca's 3DEC modelling (see later). Note that the discontinuous nature of the jointing shown in Fig. 9 was achieved by having numerically glued sections of the joints.

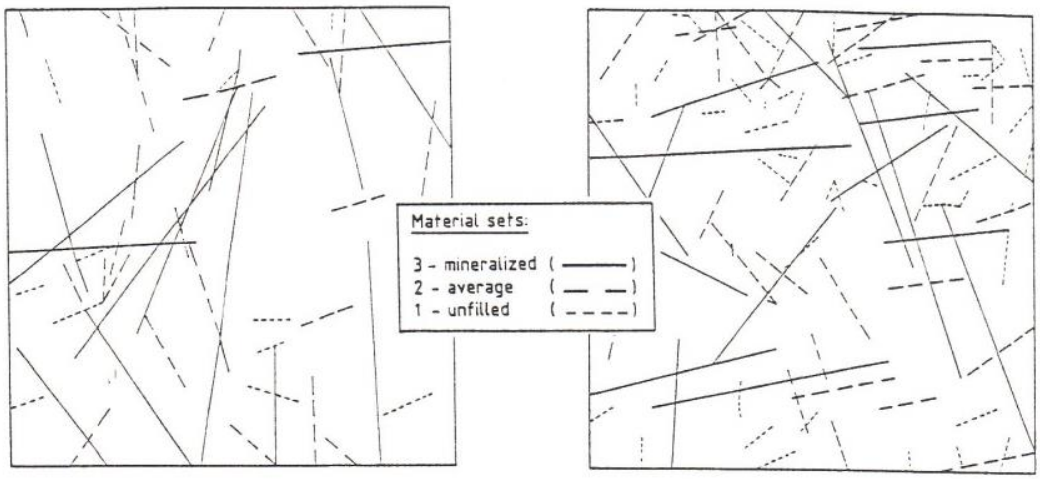

Fig. 9. Joint geometries assumed for models 1 and 4 (with average No. 2 material properties). The same geometries were used for models 5 and 8 (with length dependent material properties Nos 1 to 3, Fig. 6).

The modelled *in situ* stresses were based on McKinnon and Carr, 1990 (TR 90-09). Horizontal and vertical boundary stresses of 18 and 10 MPa were applied in the UDEC-BB models. The lower boundary of the model was a roller boundary. Simulations were performed under plane strain conditions (i.e., no deformation in the third dimension).

In the case of the coupled hydro-mechanical modelling, the *in situ* joint pressure was initially set to 2.27 MPa at the model boundaries. After the drift excavation, this pressure was reduced to 0.4 MPa at the model boundaries to approximately satisfy measured gradients (Herbert, 1989).

MECHANICAL RESPONSE

Key features of the mechanical (non-coupled) UDEC-BB modelling have been described by Barton et al., 1992 (TR 92-12) and can be summarised as follows:

1) Initial apertures of joint types No. 1, 2 and 3 were approximately 40, 25 and 1μm or less prior to excavation.
2) Excavation caused some joint shearing (generally 0.3 to 0.9mm) and some channel formation at block corners, mostly in the first 0.5m. Maximum channel dimensions ranged from almost 0.6mm at 0.4m, to 0.15mm some 1.5m inside the walls.
3) Channels can possibly provide local increases in axial permeability in the first half diameter (0 to 1.5m).
4) Peak tangential stresses of 55, 74, 64 and 62 MPa were registered in Models 5, 6, 7 and 8, while a continuum model registered a maximum tangential stress of 43 MPa (compared to virgin stresses of σ_v = 10 MPa and σ_h = 18 MPa).

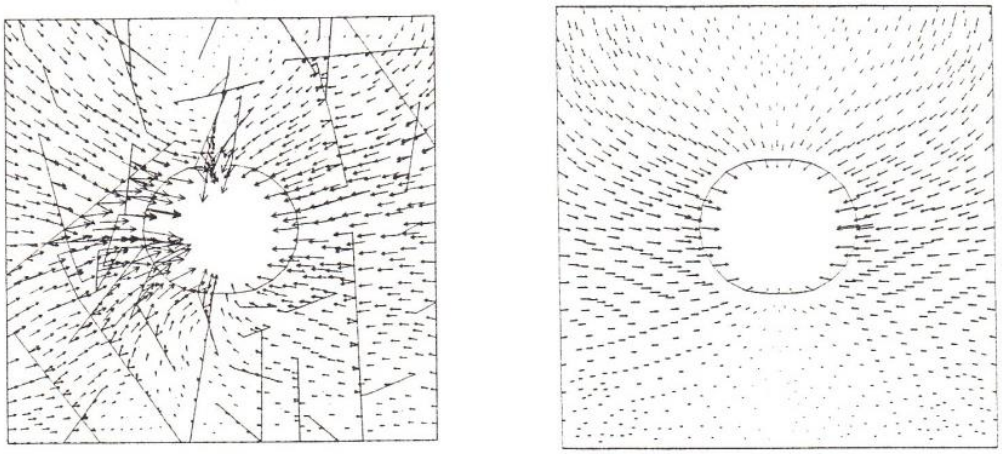

Fig. 10. Displacement vectors in jointed model No. 5 compared with the continuum model. Maxima were 1.55 and 0.75mm.

5) Joint planes intersecting the drift tend to be closed by the increased tangential stress levels (or do not shear enough to dilate) and will therefore tend to cause reduced radial permeability.
6) Excavation induced deformations showed maxima of 1.1 to 1.6mm in Models 1, 2, 3 and 4, and maxima also of 1.0 to 1.6mm in Models 5, 6, 7 and 8. Drift closures were therefore generally limited to 2 to 3mm (see Figure 10).
7) Deformations were greatest in the more jointed zones of the models, and the level of tangential stress was lower in these same jointed zones.
8) Significantly larger magnitudes of joint shearing were seen in the three-material models (5 to 8) at some 2 to 3 metres (2R) from the drift, due to the reduced shear strength of the persistent mineralized joints.
9) In these small drift simulations (3m span × 2m height) most of the disturbed zone (zone of changed apertures) was of nearly the same thickness as the assumed blast-damaged zone. This will not be the case when excavation dimensions are increased.

HYDRO-MECHANICAL (H-M) RESPONSE

Key features of the coupled hydro-mechanical UDEC-BB modelling have been described by Monsen et al., 1992 (TR 92-11) and Barton et al., 1992 (TR 92-12) and can be summarised as below:

A. D-hole Simulations (H-M model)

1. The modelling of water flow to the D-holes that were drilled around the future periphery of the future drift was limited to one model (Model 8 geometry).
2. Poorly connected parts of the model joint network showed high residual pore pressures.

3. Due to the presence of some extremely tight (material 3) joints with conducting apertures less than 1μm, time steps had to be very small and calculation times correspondingly larger. Analysis of results of D-hole excavation in Model 8 indicated that even at 300,000 cycles flow transients still existed, but mechanical equilibrium appeared to have been reached.
4. At 60,000 calculation cycles, inflow to the D-holes from two joints with connection to the boundary showed approximately $4 \times 10^{-12} m^3/sec$ (0.004 litres/sec, or 0.24 litres/min. per 1m length of D-holes).
5. At 300,000 cycles, the inflow to the D-holes from the same two joints had reduced to half the above values, i.e., to 0.12 litres/min. per 1m length of D-hole.

B. Drift Excavation (H-M Models)

Figure 11 shows results from one of the H-M drift excavation models. In general:

1. H-M models (5 and 8) showed stress rotations and moderate reductions in ***stress*** in the neighbourhood of the drifts, but occasional extra high values of stress compared to the M (uncoupled behaviour) models. (Model 8: maximum stresses M 61.9 MPa, H-M 82.2 MPa.)
2. H-M models (5 and 8) showed some general 10 to 30% reductions of ***displacements*** and some rotations in the walls, but individual maximum displacements in the arch and invert were between 120 and 140% of those in the uncoupled models. (Model 8: maximum displacements M 1.32mm, H-M 1.61mm.)
3. H-M models (5 and 8) showed some local 40 to 60% reduction and some local 20 to 40% increases in ***joint shearing***, compared to the uncoupled models. (Model 5: maximum joint shearing M 0.97mm, H-M 1.26mm.)
4. H-M models (5 and 8) showed few changes to "far-field" ***apertures***, but close to the drift some major apertures were 20 to 100% larger than in the uncoupled models. (Model 8: maximum apertures M 0.29mm, H-M 0.54mm.)
5. In general, maximum deformations, stresses, joint shearing and apertures tended to be somewhat larger in the H-M models. There were, however, exceptions.

C. Comparison of D-hole and Drift Excavation H-M Models

1. The whole D-hole model showed ***stresses*** of almost original magnitude (approx. 18 MPa horizontally, and 10 MPa vertically) while the drift excavation showed much greater anisotropy (ratio of tangential to radial stress in the range 5 to 10 or more in the first 0.5 to 0.75m from the drift walls). Maximum Stresses Model 8 D-hole (H-M) = 24.0 MPa, Model 8 Drift (H-M) = 82.2 MPa.
2. The ***displacements*** in the D-hole simulations were generally 1 to 2 orders of magnitude less than in the drift simulations, in the future drift region.

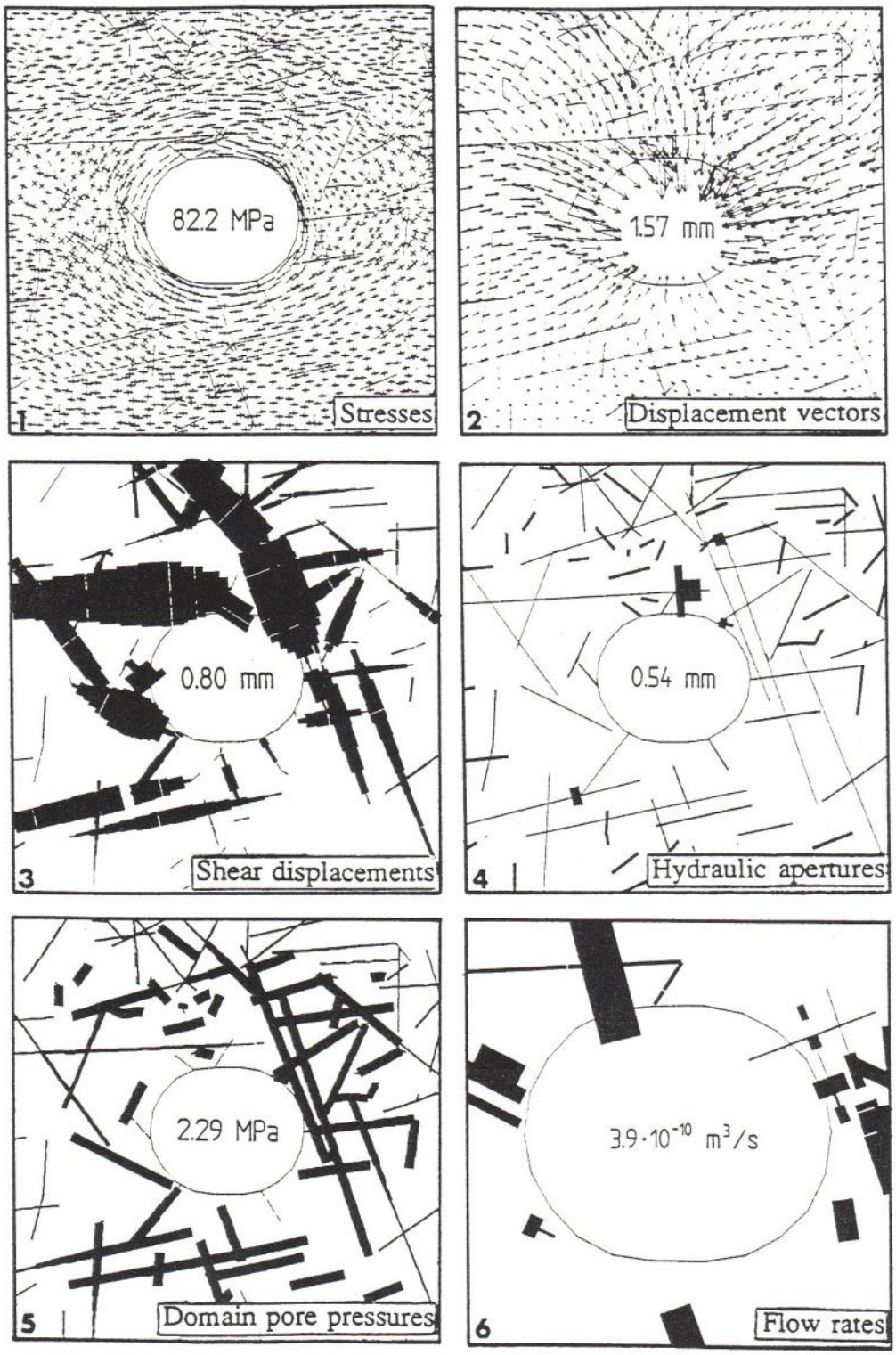

Fig. 11. Validation drift excavation with Model 8 jointing, using fully coupled H-M version of UDEC-BB.

However, the upper boundary in the D-hole simulation was displaced about 0.4mm as a result of the pore pressure reduction. Maximum Displacements Model 8 D-hole (H-M) = 0.4mm, Model 8 Drift (H-M) = 1.6mm.

3. Large differences in ***joint shearing*** were evident between the D-hole and drift simulations. Maximum shearing in the D-hole model occurred out at the boundary between the jointed discrete element zone and the surrounding boundary element (continuum) zone. Maximum shearing (at least an order of magnitude larger) occurred closest to the drift. Maximum Joint Shearing Model 8 D-hole (H-M) = 0.096mm, Model 8 Drift (H-M) = 0.80mm.
4. Out at the boundaries of both models, joint ***apertures*** appeared to be identical. However, intersections close to the drift were of course affected by the excavation and showed local major increases, especially in the arch and right-hand wall. Connectivity was however not necessarily improved by these local channels. Minimum apertures were 1μm or less in both models. Maximum Apertures Model 8 D-hole (H-M) = 0.043mm, Model 8 Drift (H-M) = 0.54mm.
5. The high tangential stresses caused by the tunnel excavation slow the dissipation of some of the high ***pore pressures***. More efficient pore pressure drainage to the D-holes was evident. Pore pressures as high as 1.6 MPa were registered in a region close to the model drift due to poor drainage through extremely tight joints.
6. With much longer running times, these extremely tight joints will drain the high pore pressures. Perhaps this modelling experience is equivalent to transients just after tunnel blasting.
7. There is evidence that the time-consuming runs with fully coupled behaviour reach equilibrium in terms of mechanical performance earlier than in the case of the flow. At 300,000 calculation cycles, the D-hole simulation in Model 8 showed 0.12 litres inflow per min. per 1m length of D-holes while the drift excavation in the same model showed 0.03 litres/min. per 1m of drift.
8. In practice, an 80 to 90% reduction in flow was observed, but inflows were about an order of magnitude less than the above. As pointed out earlier, the 2D models unfortunately could not represent the predominant jointing that was perpendicular to the drift.

THREE-DIMENSIONAL MODELLING WITH 3DEC

In an attempt to find additional reasons for the surprising reductions in inflow to the validation drift, a three-dimensional model was commissioned. Itasca Inc. utilised 3DEC, their three-dimensional discrete element code, and managed to model a selection of the more major joints including those of Set B, which in the H-zone caused most inflow. (More than 99% of the flow emanated from this zone, 57% coming from a single 2m^2 area. Flow from the "average rock" was so small that it could only be detected by evaporation/ventilation measurements; Harding and Black, 1992.)

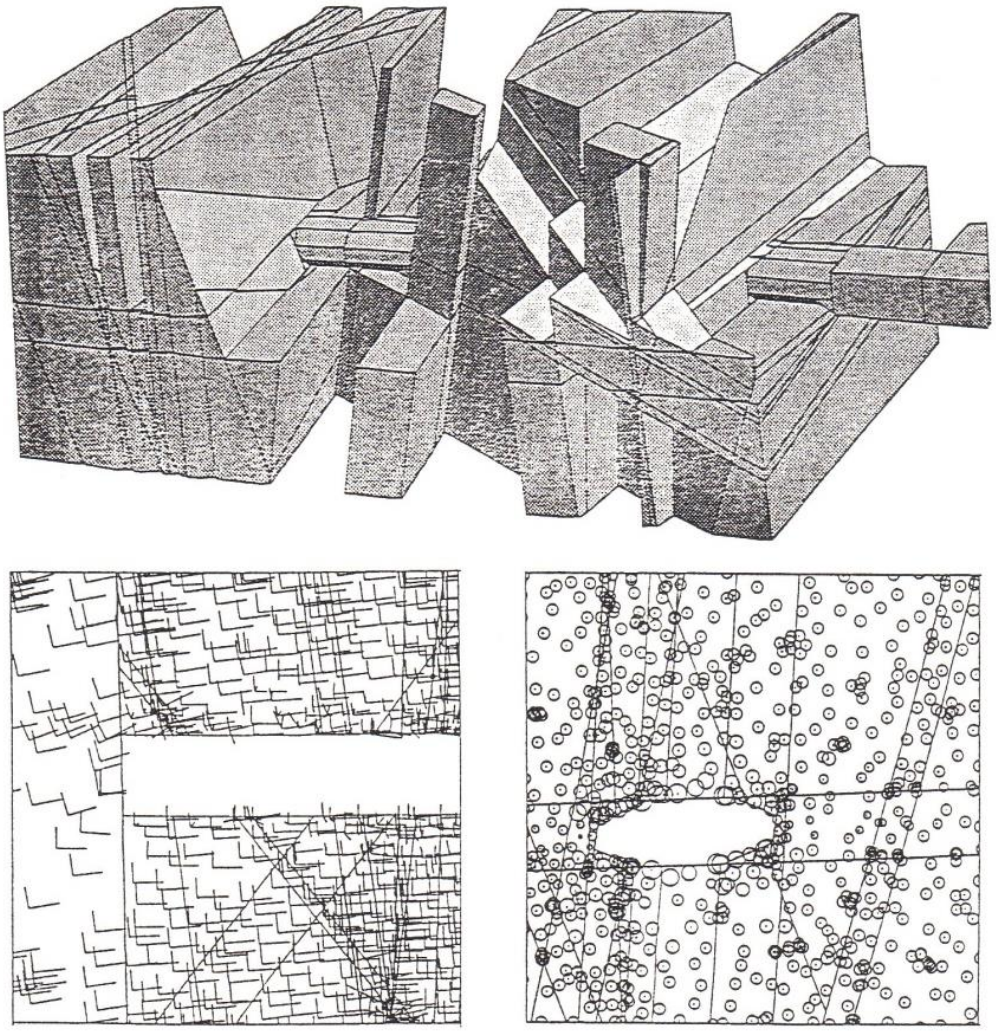

Fig. 12. 3DEC results for Validation Drift, showing cut-away 3D view (from 67°/165°), principal stresses (max. 57.9 MPa), and normal stress increases on a steep joint plane 5m from the face. (Tinucci and Israelsson, 1991)

Figure 12 shows a selection of Itasca's 3DEC results for the Validation Drift (Tinucci and Israelsson, 1991). The right-hand lower figure shows normal stresses on an oblique, steeply dipping joint about 5m from the face. Note the increased diameter of the normal stress circles on the joint plane closest to the face, which indicates at least a doubling of stress magnitude compared to the far-field stress. This of course can explain some of the observed flow reduction compared to the D-holes, but it is not a sufficient explanation. Disturbance of flow channels by block shearing is perhaps also required.

CONCLUSIONS

1. Two-dimensional modelling is obviously limited to the joints that strike parallel or sub-parallel to the axis of the modelled tunnel, in this case Sets A and C. Conclusions from the UDEC-BB modelling must therefore be used with caution in interpreting the three-dimensional behaviour of the drift.
2. Coupled H-M modelling cannot at present be performed with 3DEC but can be used in UDEC-BB. Consequently it is wise to perform both types of analysis for obtaining the best presently available understanding of how jointed rock masses behave. An essential ingredient in this understanding is the performance of coupled stress-closure-shear-dilation-flow tests on dominant joints, preferably at laboratory (CSFT) scale and on larger block tests *in situ*. Characterisation is essential in placing the results in the correct statistical perspective.
3. Several items of evidence for possibly explaining reduced inflow to the small, 3m × 2m × 50m validation drift have been unearthed by the comprehensive rock mechanics testing and modelling performed. The following items can stand alone, or can complement other explanations of possible disturbance by blasting, blast gasses, or two-phase flow (degassing).
4. The 1m × 1m × 2m block test on a mineralized, chlorite-bearing Stripa joint showed that moderate increases of normal stress (3 to 7 MPa) could diminish joint permeability to below measurable levels. Moderate levels of shearing (1.8mm) under a 10 to 11 MPa normal stress did not re-establish measurable permeability due to the joint planarity and block size.
5. CSFT tests on smaller 200mm joint samples showed significantly reduced permeabilities with stress and with time, following normal stress cycling and shearing of about 1mm. Creep of the joint infill material under increased load and/or shearing could have been a common occurrence in the newly excavated validation drift.
6. The UDEC-BB models, although limited to two-dimensions, do show reduced apertures and inefficient pore pressure dissipation for the near-field joints that are highly stressed by the excavation. Shear magnitudes in the 3m × 2m drift (0.3 to 0.9mm) were not sufficient to mobilise dilation. Potentially increased permeability was therefore only evident in an axial sense, due to channel formation at block corners. Block shearing in 2D could displace flow channels in the third dimension, i.e., in the H-zones.
7. Maximum stresses were twice as high in the jointed H-M model as compared to the continuum model (82.2 MPa compared to 43 MPa), so isotropic elastic models need cautious application.
8. Set B joints crossing the validation drift nearly at right angles (as for Zone H) were shown in 3DEC studies to bear at least a 100% increase in normal stress in the first 0.5 to 1m from the drift.

9. Closure-shear-flow (CSF) coupling along the mineralized joints at Stripa can therefore readily explain the principal SCV phenomenon of reduced flow to the drift. Geotechnical modelling should be used to actively supplement uncoupled, but three-dimensional geohydrological (network) modelling in future programmes.

REFERENCES

Bandis, S., A. Lumsden and N. Barton, 1981, "Experimental studies of scale effects on the shear behaviour of rock joints", Int. J. of Rock Mech. Min. Sci. and Geomech. Abstr. 18, pp. 1-21.

Bandis, S., A.C. Lumsden and N. Barton, 1983, "Fundamentals of Rock Joint Deformation", Int. J. Rock Mech. Min. Sci. and Geomech. Abstr. Vol 20, No. 6, pp. 249-268.

Barton, N. and V. Choubey, 1977, "The shear strength of rock joints in theory and practice", Rock Mechanics, Springer, Vienna, No. 1/2, pp. 1-54. Also NGI-Publ. 119, 1978.

Barton, N., 1982, "Modelling rock joint behaviour from *in situ* block tests: Implications for nuclear waste repository design", Office of Nuclear Waste Isolation, Columbus, OH, 96 p., ONWI-308, September 1982.

Barton, N. and S. Bandis, 1982, "Effects of Block Size on the Shear Behaviour of Jointed Rock", Keynote Lecture, 23rd U.S. Symposium on Rock Mechanics, Berkeley, California.

Barton, N., S. Bandis and K. Bakhtar, 1985, "Strength, Deformation and Conductivity Coupling of Rock Joints", Int. J. Rock Mech. & Min. Sci. & Geomech. Abstr. Vol. 22, No. 3, pp. 121-140.

Barton, N., A,. Makurat, K. Monsen, G. Vik and L. Tunbridge, 1992, "Rock Mechanics Characterization and Modelling of the Disturbed Zone Phenomena at Stripa", SKB Stripa Project TR 92-12.

Cundall, P.A., 1980, "A generalized distinct element program for modelling jointed rock. Report PCAR-1-80. Peter Cundall Associates; Contract DAJA37-79-C-0548, European Research Office, U.S. Army.

Gale, J. and A. Stråhle, 1988, "Site Characterisation and Validation - Drift and Borehole Fracture Data Stage I", SKB Stripa Project IR 88-10.

Gale, J., R. MacLeod and P. LeMessurier, 1990a, "Site Characterisation and Validation - Measurement of Flowrate, Solute Velocities and Aperture Variation in Natural Fractures as a Function of Normal and Shear Stress, Stage 3", SKB Stripa Project TR 90-11.

Gale, J. R. MacLeod, A. Stråhle and S. Carlsten, 1990b, "Site Characterisation and Validation - Drift and Borehole Fracture Data, Stage 3", SKB Stripa Project IR 90-02

Hakami, E., 1989, "Water Flow in Single Rock Joints", SKB Stripa Project TR 89-08.

Harding, W., and J. Black, 1992, "Site Characterization and Validation - Inflow to the Validation Drift", SKB Stripa Project TR 92-14.

Herbert, A., 1989. Private Communication.

Makurat, A., N. Barton, L. Tunbridge and G. Vik, 1990a, "The measurement of the mechanical and hydraulic properties of rock joints at different scales in the Stripa project", International Symposium on Rock Joints. Loen 1990. Proceedings, pp. 541-548, 1990.

Makurat, A., N. Barton, G. Vik, P. Chryssanthakis and K. Monsen, 1990b, "Jointed rock mass modelling", International Symposium on Rock Joints. Loen 1990. Proceedings, pp. 647-656, 1990.

McKinnon, S. and P. Carr, 1990, "Site Characterization and Validation - Stress Field in the SCV Block and Around the Validation Drift, Stage 3", SKB Stripa Project TR 90-09.

Monsen, K., N. Barton and A. Makurat, 1992, "Fully-Coupled Hydro-Mechanical Modelling of the D-Holes and Validation Drift Inflow, SKB Stripa Project TR 92-11.

Tinucci, J.P., and J. Israelsson, 1991, "Site Characterization and Validation - Excavation Stress Effects Around the Validation Drift. SKB Stripa Project, TR 91-20.

Vik, G. and P.M. Johansen, 1990, "Determination of shear strength of rock joints at two dam sites and at Stripa Research Mine", International Symposium on Rock Joints. Loen. Proceedings, 1990.